MACRO AND MICROSEGREGATION ASSESSMENT METHOD FOR CONTINUOUS CASTING OF WIDE SLABS*

Gilberson Mendonça Storck de Melo[1]
Afranio Márcio Costa[2]
André Afonso Nascimento[3]
Alisson Paulo de Oliveira[4]
Antonio Augusto Gorni[5]
Gabrielly Lorraine Pereira de Oliveira[6]
Jose Maria Rodriguez-Ibabe[7]

Abstract

Macro and micro segregation play a key role in understanding the solidification behavior of continuously cast steels. Both affects directly critical applications, which requires a higher degree of homogeneity since as cast stage. This study applied macro and micro approaches to perform a comprehensive characterization of the solidification microstructure for wide slabs. In the macro-approach, a width-wise chemical analysis was performed using OES on whole centerline. Thickness-wise analysis was also implemented at 300 mm intervals in width direction. Carbon content in centerline was almost three times higher than base chemistry. The same behavior happened with P, S, Ti, and Nb. The micro-approach in this study considered SDAS (Secondary Dendrite Arm Spacing) and second phase particles. Calculated figures presented particularly good correspondence with measured ones for both micro-approach features. *Liquidus* and *solidus* position, as well as mushy zone were calculated using CON1D model. NbC and MnS were the most relevant second phase particles calculated by Factsage. This finding matches to the analysis carried out by SEM-EDS. Based on these results, which measured values were in good agreement with calculated ones, it is possible to estimate the internal quality of slabs in a higher degree of confidence.

Keywords: continuous casting; centerline segregation; solidification microstructure.

1 *Metallurgical Engineer, M.Sc., Researcher, R&D/Steel Technology department, Gerdau – Ouro Branco steel works, Ouro Branco, MG, Brazil.*
2 *Metallurgical Engineer, M.Sc., Manager, R&D/Steel Technology department, Gerdau – Ouro Branco steel works, Ouro Branco, MG, Brazil.*
3 *Metallurgical Engineer, M.Sc., Process Specialist, Continuous Casting/Melt Shop, Gerdau – Ouro Branco steel works, Ouro Branco, MG, Brazil.*
4 *Metallurgist Engineer, D.Sc., Consultant, CBMM, São Paulo, MG, Brazil.*
5 *Materials Engineer, D.Sc., Consultant, CBMM, São Paulo, MG, Brazil.*
6 *Undergraduate Student, School of Engineering/Metallurgical Engineering department, UFMG, Belo Horizonte, MG, Brazil.*
7 *Industrial Engineer, Ph.D., Executive President, CEIT, Donostia/San Sebastian, Guipuscoa, Spain.*

** Technical contribution to the 52º Seminário de Aciaria, Fundição e Metalurgia de Não-Ferrosos, part of the ABM Week 7th edition, August 1st-3rd, 2023, São Paulo, SP, Brazil.*

1 INTRODUCTION

As has already been widely reported in the technical literature, the segregation that occurs in the continuous casting of steels can be on a microscopic scale, arising from the last liquid that solidifies between the dendrites, and on a scale like that of the strand, in its core, which are respectively designated as being micro and macrosegregation. It is virtually impossible to eliminate the distribution of alloy element concentrations established by the segregation that occurs during solidification, which ends up being inherited even by successively hot-rolled, cold-rolled and annealed flat products [1]. The most common manifestation of this pattern is the presence of microstructure banding, that is, alternating longitudinal bands of ferrite and pearlite. The costly normalizing heat-treatment can remove pearlite banding, but it is noncapable to fully remove the micro-segregation pattern in the alloy [2]. The lack of segregation control can strongly impact the performance of the final steel product in the most diverse ways [3].

The continuous evolution of the quality of steel products, together with the pressure to reduce their costs, motivated the execution of numerous studies aimed at understanding and modeling the metallurgical phenomena associated with segregation. One of the most remarkable works in this sense was developed by Won and Thomas [4], based on the Clyne-Kurz model [5] and which is part of the global model for one dimensional heat transfer and solidification during continuous slab casting, CON1D [6], which has been continuously improved over the past decades by the Continuous Casting Consortium. Another alternative that has been widely used recently is the simulation of solidification and the consequent segregation using computational thermodynamics packages, such as ThermoCalc and FactSage. Artificial Intelligence is also being used in this context [7].

A previous study, carried out cooperatively between Gerdau Ouro Branco and CBMM, characterized the influence of micro-segregation on the formation of the microstructure and, particularly, the size distribution of microalloy precipitates in the interdendritic region of the plates [8]. This last work, constitutes the starting point for more specific studies on continuous casting of slabs, now also involving the Continuous Casting Consortium (CCC). In the present work, the centerline segregation that occurs in the continuous casting of slabs at this plant was characterized in detail.

2 TESTING METHODS

2.1 Macro analysis

An industrial experiment was performed on a continuously cast HSLA Nb-Ti microalloyed grade. A sample was taken from tundish after homogenization. **Table 1** shows details of chemical composition that, hereafter, will be nominated as “base chemistry”. Among the elements in steel chemical composition, this present work selects the six more relevant elements for segregation. This pick considers the partition and diffusion coefficients in delta ferrite and austenite [9].

Table 1. Base chemistry of test heat – mass content in %wt

C	Mn	Nb	Ti	P	S
0.15	1.35	0.026	0.015	0.021	0.005

Test heat produced 250mm x 2107mm slab. During the casting, a sample of 80mm long was taken. After air cooling, the slab sample was cut into 07 pieces, according to **figure 1a**, and then ground and etched with HCl to reveal slab macrostructure and its centerline segregation. After that, smaller pieces were cut in thickness-wide and width-wide strategy for five macro-etch samples as stated in **figure 1a**. These pieces were ground again and sent to an Optical Emission Spectrometer (OES) to analyze the chemical composition at the points defined in **figure 1b** and **1c**. The main goal was to determine the differences between the base chemistry shown in **table 1** and local chemical composition.

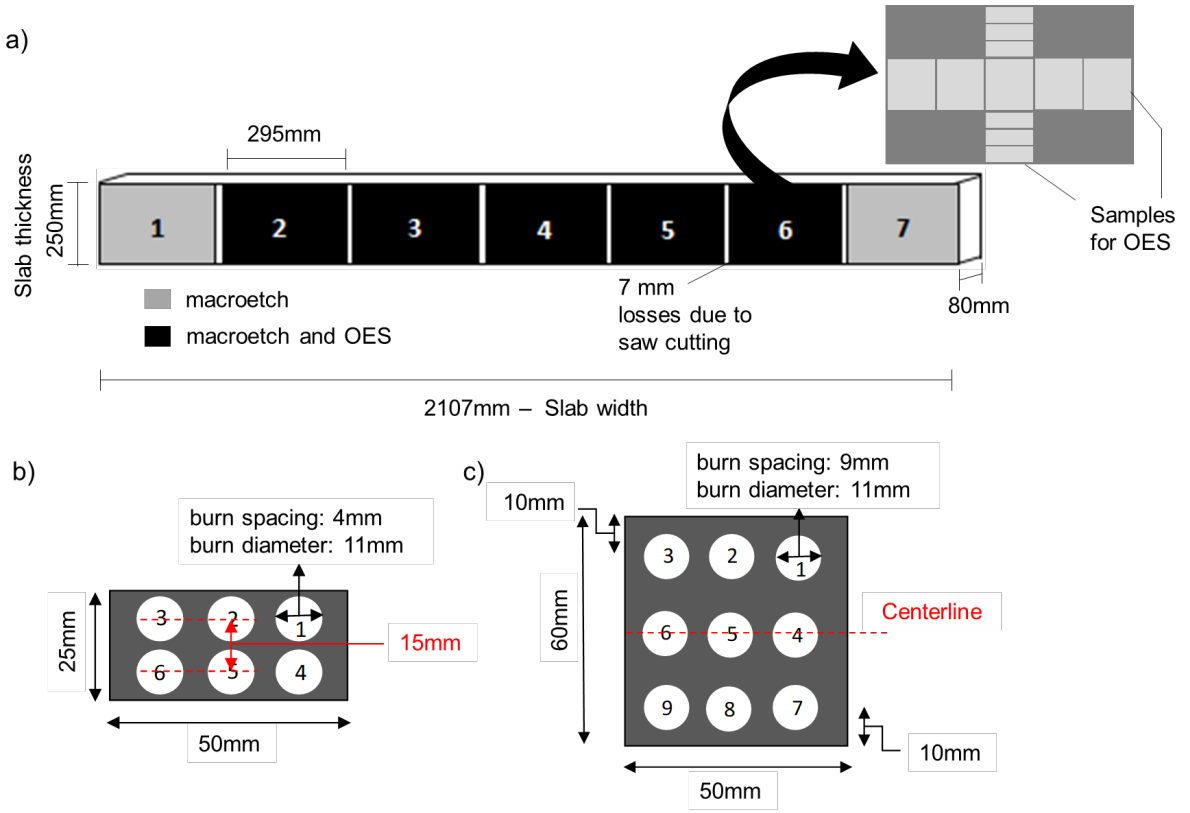

Figure 1. (a) Samples for macro-etch taken from slab width, detailing smaller samples for OES. (b) Thickness-wide sample for OES. (c) Width-wide sample for OES. Numbers 1 to 6 in (b) and (c) means individual OES burns.

2.2 Micro analysis

After identifying the fields of higher concentration that define centerline segregation, among the samples 2 – 6 (**figure 1a**), it was selected two samples: one that has fields with higher concentration and another one without pronounced segregation. Metallography for determination of steel matrix features and dendritic microstructure was carried out on samples at 37.5mm below slab top surface (inner radius) and centerline to compare the differences between last portion to solidify (centerline) and an intermediate point. For that, two different etchants were used: Nital 2%, for the first
determination and Picral 2% for second one.

2.1.1 SDAS measurements

During the solidification process, solid dendrites and interdendritic liquid coexist at mushy zone. Segregation pattern is largely influenced by microstructural length scales of dendrites, especially secondary dendrite arm spacing (SDAS) [10]. This

present work measured and calculated the SDAS. The first one was done by intercept method using optical micrographs taken by metallurgical microscope instrumented with CCD camera and proper image analysis software. SDAS calculation is described in next section

2.2.2 Second phase particles in centerline

Once there is less solubility for solutes in the solid compared with that in the liquid phase, concentrations of these elements in the primary solid are lower than in the liquid. Considering that mentioned process is continuously repeated until the end of solidification, slab centerline is the portion not only solute-richer but also the region where second microscopic phase particles lie after being pushed by solidification front. SEM-EDS analysis was performed to identify second phase particles in centerline.

3 CALCULATIONS

3.1 Secondary Dendrite Arm Spacing (SDAS)

Several empirical relationships have been reported elsewhere [11], and almost all of them made a relationship with solidification time or cooling rate. Some of them also reported influence of carbon content as an argument of their equations [4, 11, 12]. Based on that, SDAS measurements can provide valuable information to estimate solidification process. This paper uses the empirical relationship reported by Won and Thomas [4] which are coupled in CON1D model [4, 6].

3.2 Mushy zone, *solidus* and *liquidus* positions

This present work applied the well know and widely reported continuous casting solidification model CON1D. Process parameters of test heat and geometrical parameters of Gerdau Ouro Branco steelworks slab caster machine were fed into the model, to have outputs like *solidus* and *liquidus* position and length of mushy zone, cooling rates and local solidification time. The last two support SDAS calculations. **Table 2** displays most relevant inputs for this calculation.

Table 2. Some relevant casting data obtained by test heat and used as input data in CON1D

Input data	value
Slab section [mm]	250 x 2107
Super heat [°C]	25
Casting speed [m/min]	0.90
Metallurgical Length [m]	36.9
Mold geometry	Straight
Mold length* [mm]	800
Roll diameter [mm]	Bender segment: 150 Bow segments: 230 Straighteners: 300
Secondary cooling spray angle [deg]	Bender segment: 105 Bow and straighteners: 110

** Mold length considers from meniscus to mold end.*

3.3 Second phase mass contents

Solidification of a multicomponent alloy was considered according to base chemistry previously defined in **table 1**. In addition to that, N = 0.0034% wt. (Nitrogen content of

test heat) and Fe = balance were also considered. Secondary phase mass contents were estimated using equilibrium cooling with back diffusion in Equilb module of FactSage 8.2. Cooling calculations were performed considering, as an assumption, that solute diffusion is infinitely fast in the liquid. Solute redistribution with rapid solid state diffusion is also considered and governed by Fick's second law. Since the solute partitioning generates substantial concentration changes and concentration gradients ahead of the solid/liquid interface [12], the option to consider back diffusion in this simulation make sense once that process aforementioned drives the back diffusion.

4 RESULTS AND DISCUSSION

4.1 Macro analysis

Figure 2 shows a concentration map for C, Mn, Nb, Ti, S and P for samples 2 to 6. Each little square represents an individual analysis, as previously seen in **figure 1**. Dark areas mean higher concentration. Virtually, there is no significant variation from slab surface up to 112mm below both surfaces (inner and outer radius).

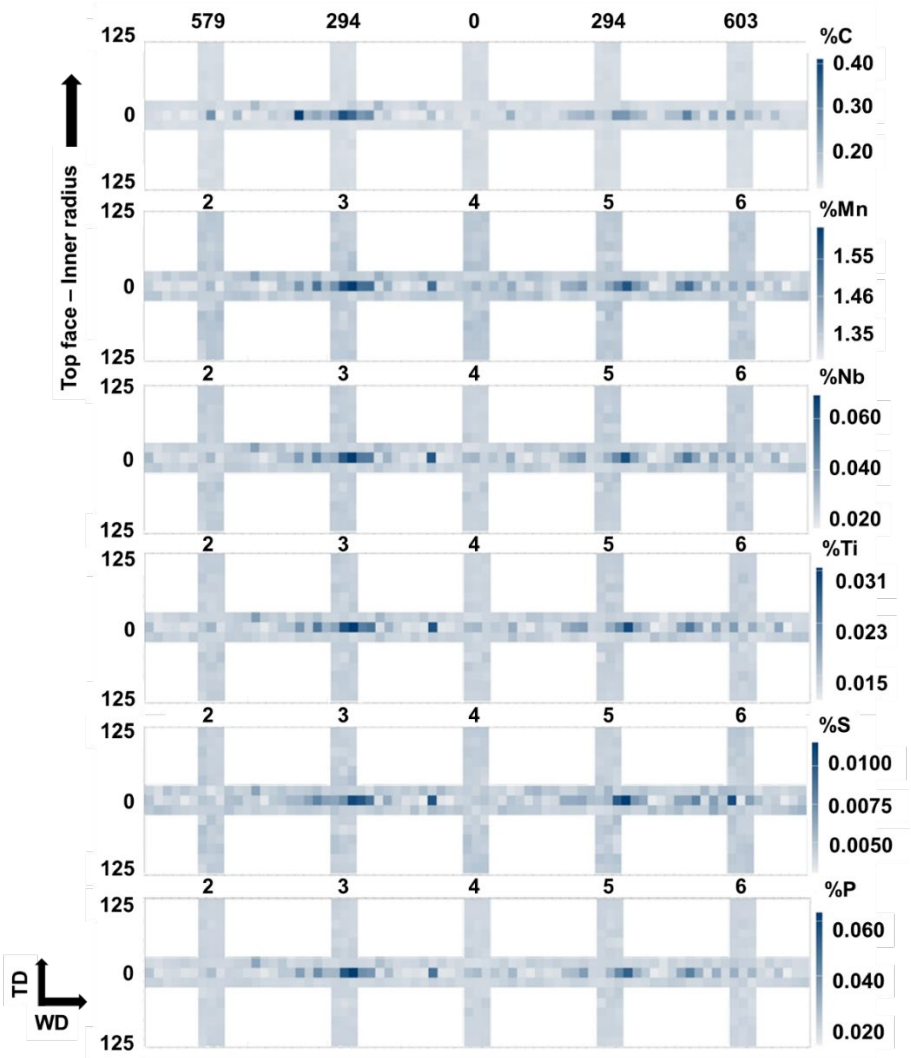

Figure 2. Concentration map for C, Mn, Nb, Ti, S and P, considering slab thickness-wise and width-wise directions. TD: Thickness Direction. WD: Width Direction. Samples 2 to 6. Thickness and width are given in millimeters.

Figure 2 also characterizes the segregation profile in transversal section of test slab. Portions with severe segregation (sample 3 and region between sample 5 and 6) probably come from the prominent parts of an irregular solidification front, as shown in **figure 3**. Once these ones are the last parts to solidify, the liquid core inside these locations are the richest one. The center of slab (sample 4) would represent the latter portion of solidification front. This part, located at the center of solidification front, is the first part to solidify and, of course, has a poorer solute concentration when compared to prominent parts. The probable solidification front could be better understood as an analogy of letter "U" as shown in **figure 3.**

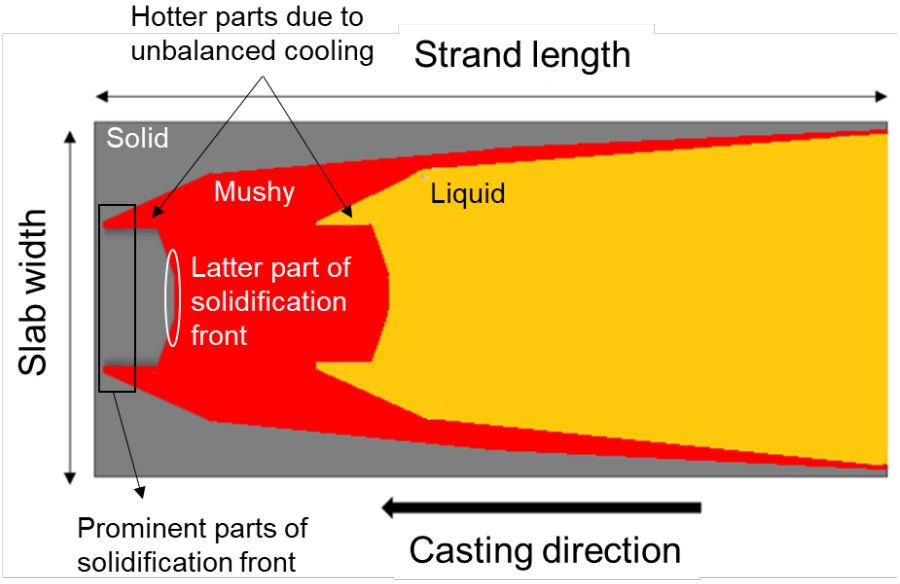

Figure 3. Probable solidification front pattern due to unbalanced cooling across slab width.

Li *et al.* [13] and Long and Chen [14] reported similar macro segregation pattern. Both authors addressed unbalanced secondary cooling on slab wide surface and unsuitable casting speed as main causes for macro segregation like reported in **figure 2**. Additionally, after soft reduction, a possible trapping of enriched final liquid present in protuberant parts of solidification front could be related to portions where severe centerline segregation was found.

With exception to Mn, the concentration of other elements can be 2 to 3 times higher than base chemistry. Although a concentration increase can be seen in centerline of sample 4 (center of width), it is just around 30% higher than base chemistry. A recent work [15] reported that increase in concentration of C, P and S in centerline segregation peak is almost the double. Another author [16] reported that an increase of 3.3 times in C concentration was found in a calculation considering solid fraction 0.99 for wide and heavy peritectic slabs with 0.13% wt. as base concentration.

4.2 Micro analysis

4.2.1 Steel matrix, constituents, and dendritic microstructure

Figure 4 and **Figure 5** show metallography of steel matrix features and dendritic microstructure respectively for sample 3, containing severe segregation and sample 4 with no relevant segregation. As it can be seen, through **figure 4**, SDAS and steel matrix at centerline segregation is quite different from intermediate portion (37.5mm). Pearlite colonies presented in **figure 4c** suggests a high carbon grade while steel matrix and constituents observed in **figure 4a** match with peritectic-medium carbon

grade of base chemistry. Solidification microstructure given by **figures 4b** and **4d** follow the same pattern. The second one, which refers to centerline segregation, presents thinner secondary dendrite arms when compared to intermediary portion. This fact influences directly SDAS measures, which is linked to higher carbon content and solute enrichment in centerline.

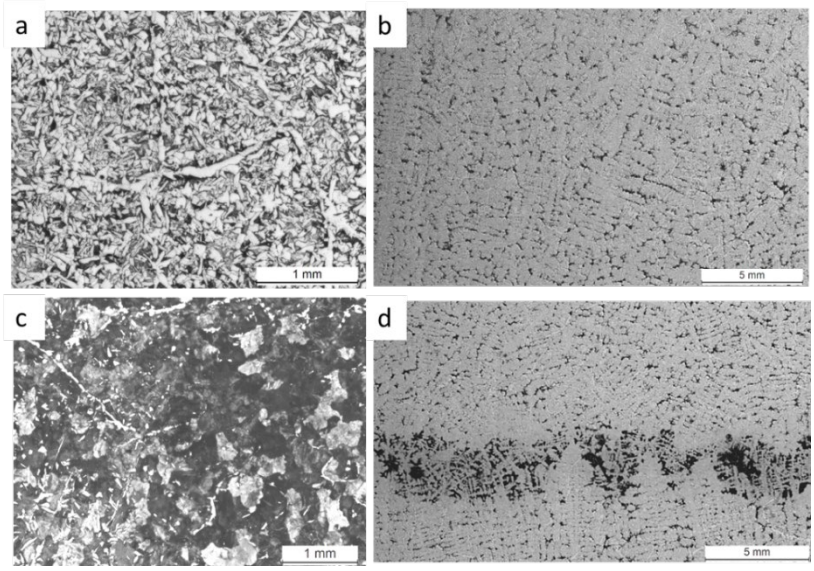

Figure 4. Microstructure of sample 3. (a) and (b) show microstructure observed at 37.5mm below top surface – inner radius. (c) and (d) microstructure observed in centerline segregation

Although a difference between intermediate position (37.5mm) and centerline could be observed in **figure 5**, there is a slight contrast between the two positions. Steel matrix and its constituents in centerline agrees well with an expected level of segregation of a regular HSLA grade with 0.15% C, without any casting issues which could decrease internal quality of slabs.

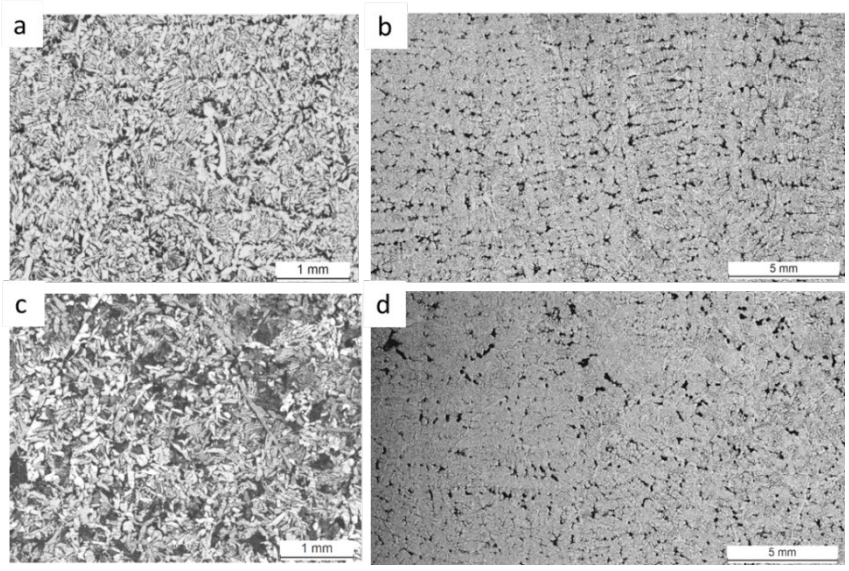

Figure 5. Microstructure of sample 4. (a) and (b) show microstructure observed at 37.5mm below top surface – inner radius. (c) and (d) microstructure observed in centerline segregation.

4.2.2 Second phase particles in centerline

Figure 6 and **figure 7** shows second phase particles found at centerline segregation, respectively for sample 3 (containing severe segregation) and sample 4 (with no relevant segregation). As mentioned before, a possible non-uniform cooling intensity across the slab width could bring an uneven solidification front, as shown in **figure 3**. In this case, it is expected that prominent parts of solidification front take place where the cooling intensity is the lowest. The liquid core inside that prominent part is the richest one, not only about solutes but also in second phase particles.

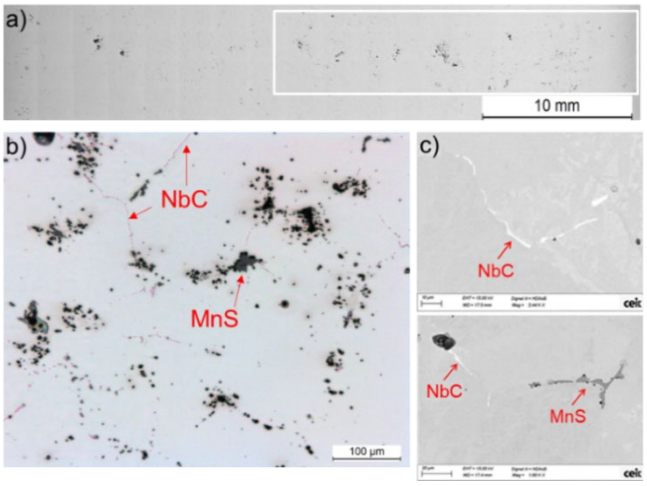

Figure 6. Second phase particles at centerline segregation – sample 3. (a) macrostructure (b) and (c) NbC and MnS dispersed in steel matrix.

Figure 6b and **6c** suggests that NbC precipitated at grain boundaries in a string form. This finding is according to Gladman [17] which defines that other forms of NbC could be expected, however they are too small to be found by an EDS. **Figure 6b** also suggests that MnS was found associated/covering, probably, oxide inclusions (black dots inside gray matter = oxide inclusions that, probably, were withdrew during grinding/polishing stage of sample preparation).

Figure 7 shows an analysis of a typical field of centerline segregation from sample 4. Once this sample comes, probably, from a latter part of solidification front, it is reasonable to expect that liquid core inside this part is poorer than prominent one. Consequently, this liquid carried lower solute concentration, as well as second phase particles when compared with liquid core of prominent part of solidification front.

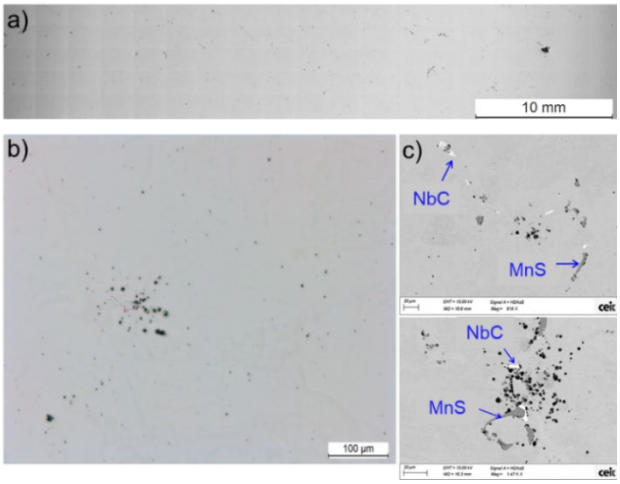

Figure 7. Second phase particles at centerline segregation – sample 4. (a) macrostructure (b) and (c) NbC and MnS dispersed in steel matrix.

The pattern of **figure 6** and **figure 7** matches with **figure 2**, i.e., higher solute concentration is associated to the presence/quantity of second particle phases. In other words, it means that macro segregation is not only about simply a solute concentration matter, but also about second particles phases.

4.3 Calculations

4.3.1 SDAS

SDAS was estimated based on actual values for water flow in primary and secondary cooling zones. Margin zones were considered to run a calculation for sample 3 and center zones were considered to run a calculation for sample 4. For the cooling practice applied for present steel grade, there is slight difference between them. **Figure 8** shows a comparative between measurements and calculation.

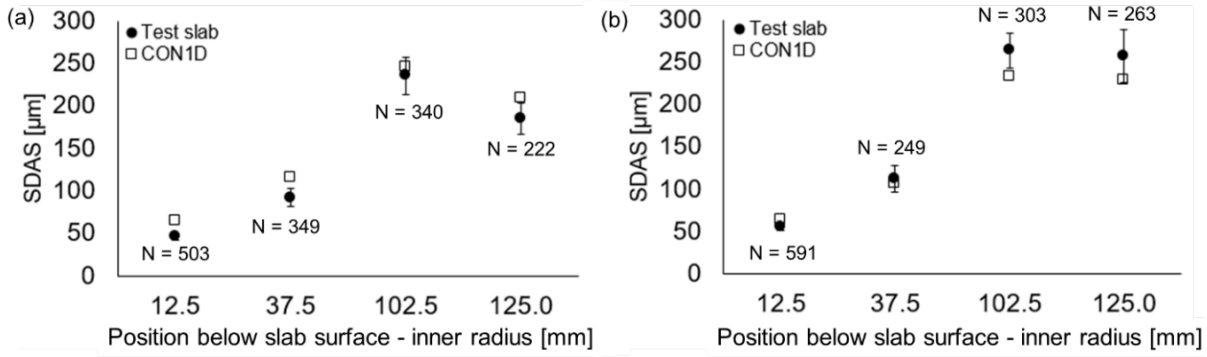

Figure 8. SDAS comparisons between Test slab and CON1D. (a) Sample 3 – severe segregation (b) Sample 4 – light segregation. Upper and lower bars mean one standard deviation of measurements (N) in test slab for each position.

CON1D results presented the same behavior as measurements performed in test slab. It was observed few differences in the SDAS calculations between the samples. The most relevant one is a considerable SDAS drop in the last two measurements and calculations observed in sample 3. This fact could be explained by liquid enrichment point of view: *liquidus* and *solidus* temperature decreases and, consequently, solidification time also decreases. As SDAS is proportional to solidification time [4, 6, 11, 12], the observed behavior is expected. The same could

be used for sample 4: The last two SDAS (102.5 and 125.0mm) was almost the same for measurements and calculations: it means that last liquid was not too much different from the 102.5mm position and, consequently, solidification time of two last positions was almost the same.

4.3.2 Second phase particles

Figure 9 shows output of cooling calculation considering equilibrium with back diffusion given by FactSage 8.2. Simulation input considered 100g of reagents/products and chemistry conditions previously stated in section 3.3.

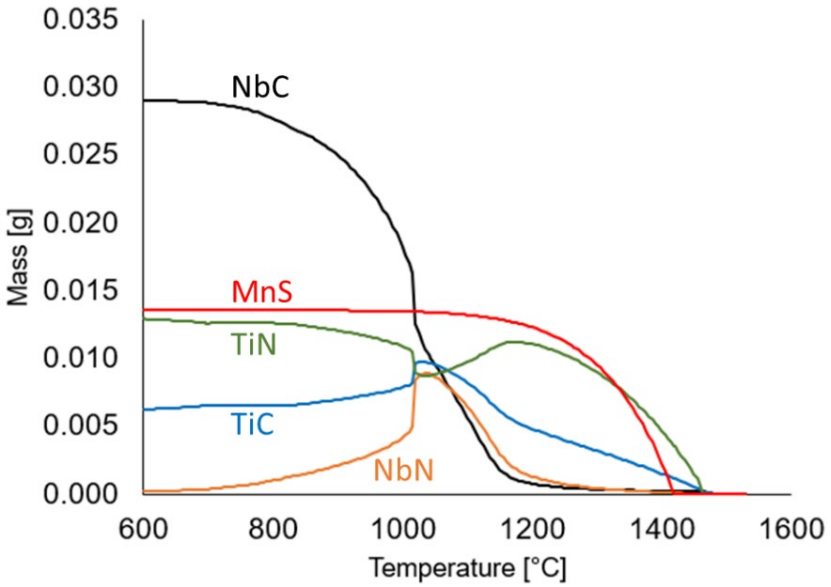

Figure 9. Second phase mass contents using equilibrium cooling with back diffusion in Equilb module of FactSage 8.2.

As it can be seen by **figure 9**, NbC and MnS were the most relevant second phase particles of the test heat. This prediction matches with what it could be seen in **figures 6 and 7**. However, the predicted TiN content was almost the same of MnS. One of possible reasons that TiN could not be seen, in mentioned figures, relies on the microscopes resolutions (Optical and SEM) used in this present work: particles less than 2µm cannot be identified accurately. Stock [18] reported that less than 10% of TiN precipitates of HSLA Nb-Ti grade cooled under a typical slab center cooling rate (0.1 °C/s - for instance, CON1D predicted for this present work 0.13 °C/s) are larger than 1µm. In this case, another equipment, like TEM or STEM should be used [18, 19].

4.3.3 Mushy zone, *solidus* and *liquidus* positions

Figure 10 represents a longitudinal view of strand mushy zone. This figure shows both *liquidus* and *solidus* positions, as well as the length of mushy zone for each case: test slab - data informed by supervisory system of continuous casting machine and CON1D simulation, which used a data set of test slab extracted by caster test server. As it can be seen, a difference of 150mm in *liquidus* position is small when compared to segments and rolls dimensions. Positions close to 14.5m in CC machine has a roll diameter with 230mm. It suggests that difference between CON1D and caster data is lower than a roll. *Solidus* position, which is more sensible to casting process and its variations, was estimated by CON1D as 730mm earlier than caster data. At 21m inside the caster, the diameter of rolls is a little bit higher:

300mm. It means that the difference between CON1D and caster data are almost 2.5 rolls. Since all segments have seven rows of rolls, the differences found for both positions are small and, based on these results, CON1D estimations were very adherent with caster industrial data.

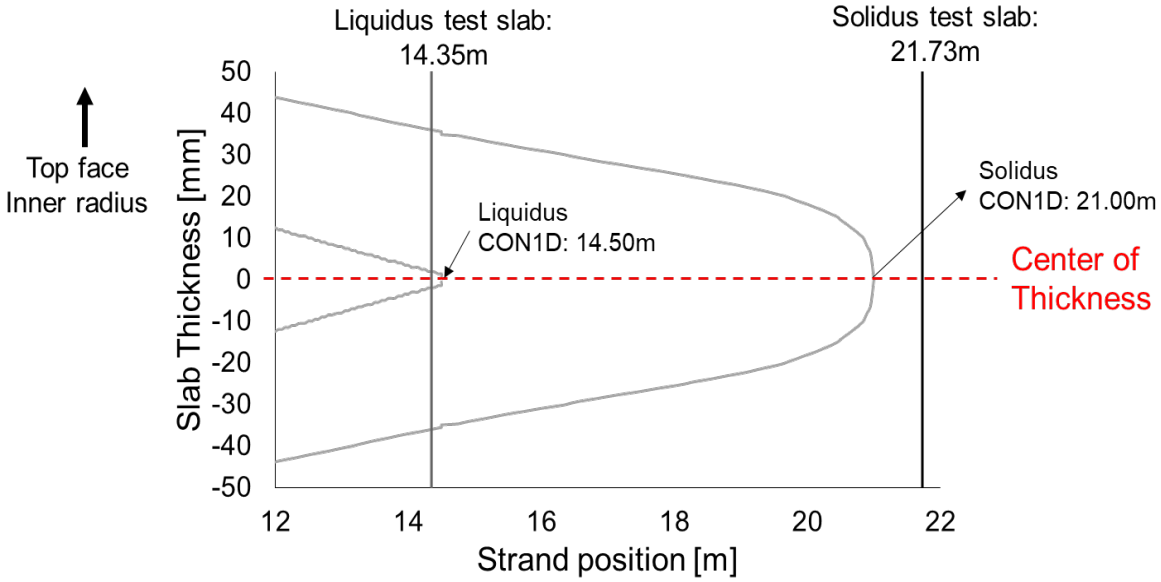

Figure 10. Representation of a longitudinal view of strand mushy zone, with *liquidus* and *solidus* point comparisons between caster data and CON1D estimations.

5 CONCLUSIONS

The method of macro and micro segregation assessment presented here has done its homework by establishing a procedure to identify and measure the intensity and segregation pattern in a wide slab. This pattern, probably, comes from an unbalanced cooling across the slab width, which leads to an irregular ("U-shape") solidification front. Higher solute concentration is linked to presence/quantity of second particle phases. In other words, it means that macro segregation is not only about simply a solute concentration matter, but also about second particles phases. CON1D present itself as a good and reliable tool for simulation, once its estimations for SDAS, mushy zone length, *liquidus* and *solidus* positions presented good agreement with measured values (SDAS) and caster industrial data.

REFERENCES

[1] Preβlinger H., Mayr M., Tragl E., Bernhard C. Assessment of the Primary Structure of Slabs and the Influence on Hot- and Cold-Rolled Strip Structure. Steel Res. Int. 2006;77:107-15.
[2] Spitizig W. Effect of sulfide inclusions morphology and pearlite banding on anisotropy of mechanical properties in normalized C–Mn steels. Metall. Trans. A. 1983;14:271-83.
[3] Lage M., Costa e Silva A. Evaluating segregation in HSLA steels using computational thermodynamics. J. Mater. Res. Technol. 2015;4(4):353-8.
[4] Won Y., Thomas B. Simple Model of Microsegregation during Solidification of Steels. Metall. Trans. A. 2001;32A:1755-67.

[5] Clyne T. W., Kurz W. Solute Redistribution During Solidification with Rapid Solid-State Diffusion. Metall. Trans. A. 1981;12A:965-70.
[6] Meng Y., Thomas B. Heat-Transfer and Solidification Model of Continuous Slab Casting: CON1D. Metall. Trans. B. 2003;34B:685-705.
[7] Zhang P., Minglin W., Shi P., Xu L. Effects of Alloying Elements on Solidification Structures and Macrosegregation in Slabs. Metals, 2022;12:1826-44.
[8] Escobar D., Castro C., Borba E., Oliveira A., Camey K., Taiss E. *et al.* Correlation of the Solidification Path with As-Cast Microstructure and Precipitation of Ti,Nb(C,N) on a High-Temperature Processed Steel. Metall. Trans. A. 2018;49A:3358-72.
[9] Zhang D. Characterization and modelling of segregation in continuously cast steel slab [thesis]. Birmingham: University of Birmingham; 2015.
[10] Straffelini G., Lutterotti L., Tonolli M., Lestani M. Modeling solidification microstructures of steel round billets obtained by continuous casting. ISIJ Int. 2011;51(9):1448-53.
[11] Weisgerber B., Hecht M., Harste K. Investigations of the solidification structure of continuously cast slabs. Steel Res. Int. 1999;70:403-11.
[12] You D. Modeling microsegregation and nonmetallic inclusion formation based on thermodynamic databases [thesis]. Leoben: Montanuniversität Leoben; 2016.
[13] Li J., Sun Y-H., An H-H., Ni P-Y. Shape of slab solidification end under non-uniform cooling and its influence on central segregation with mechanical soft reduction. Int. J. Miner. 2021;28(11):1788-98.
[14] Long M., Chen D., Study on Mitigating Center Macro-Segregation During Steel Continuous Casting Process. Steel Res. Int. 2011;82:847-56.
[15] Quinelato F., Garção W., Paradela K., Sales R., Baptista L., Ferreira A. An Experimental Investigation of Continuous Casting Process: Effect of Pouring Temperatures on the Macrosegregation and Macrostructure in Steel Slab. Mater. Res. 2020;23(4):1-9.
[16] Wang W., Zhu M., Cai Z., Luo S., Ji C. Micro-Segregation Behavior of Solute Elements in the Mushy Zone of Continuous Casting Wide-Thick Slab. Steel Res. Int. 2012;83:1152-62.
[17] Gladman T. The Physical Metallurgy of Microalloyed Steels. The Institute of Materials; 1997.
[18] Stock J. NbC and TiN Precipitation in Continuously Cast Micro Alloyed Steels [thesis]. Golden: Colorado School of Mines; 2014.
[19] Muller C-E. Precipitation during continuous casting [dissertation]. Berlin: Technischen Universität Berlin; 2015.